ACS NANO

www.acsnano.org

PERSPECTIVE

Atomic-Scale Dynamics Probed by Photon Correlations

Anna Rosławska,*,‡ Christopher C. Leon,‡ Abhishek Grewal, Pablo Merino, Klaus Kuhnke,* and Klaus Kern

Cite This: *ACS Nano* 2020, 14, 6366–6375

Read Online

ACCESS | Metrics & More | Article Recommendations | Supporting Information

ABSTRACT: **Light absorption and emission have their origins in fast atomic-scale phenomena. To characterize these basic steps (*e.g.*, in photosynthesis, luminescence, and quantum optics), it is necessary to access picosecond temporal and picometer spatial scales simultaneously. In this Perspective, we describe how state-of-the-art picosecond photon correlation spectroscopy combined with luminescence induced at the atomic scale with a scanning tunneling microscope (STM) enables such studies. We outline recent STM-induced luminescence work on single-photon emitters and the dynamics of excitons, charges, molecules, and atoms as well as several prospective experiments concerning light−matter interactions at the nanoscale. We also describe future strategies for measuring and rationalizing ultrafast phenomena at the nanoscale.**

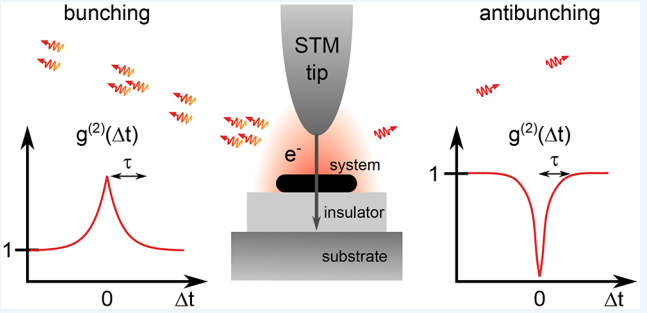

Light−matter interactions at the atomic scale are crucial to many branches of science. They constitute the basis of quantum optics, determine the efficiency of electroluminescent or photovoltaic devices, or drive photochemical processes. Fundamental understanding of such mechanisms, which is necessary for both upscaling and improving several technologies, requires direct interrogation of individual events and entities, such as how single charge-transfer events and photons interconvert and how single molecules move and undergo chemical reactions. These processes can be very fast. Routine probes of such effects involve luminescence and ultrafast laser spectroscopy, with the latter reaching the subfemtosecond regime.[1,2] However, for free propagating beams, both probes are diffraction limited, so their spatial resolution is restricted to a few hundred nanometers. This scale is 2−3 orders of magnitude above the spatial dimensions of the molecular and atomic-scale emitters of interest in this Perspective. Alternatively, scanning probe and electron microscopies permit studying emitters with even picometer precision, albeit for relatively slow (millisecond) dynamics. Recently, these techniques have also been developed for ultrafast time scales,[3,4] especially in the field of scanning tunneling microscopy (STM), in which researchers have successfully combined atomic-scale studies with time-resolved optics-based methods.[5−10] In this Perspective, we focus on the combination of STM-induced luminescence (STML) with time-resolved light detection without employing laser pulses. This partnership provides experimentalists with unique access to the dynamics of important physical processes, such as the charge transport, molecular motion, or quantum properties of light, all achieved by studying photon correlations that originate from picosecond−picometer phenomena. We present recent advances in this rapidly developing field and describe possible experiments that may further broaden our understanding of light−matter interaction dynamics at the atomic scale.

> In this Perspective, we focus on the combination of scanning tunneling microscopy-induced luminescence with time-resolved light detection without employing laser pulses.

PHOTON CORRELATIONS IN PRACTICE

Because of wave−particle duality, a light beam can be considered as a stream of photons. The temporal statistics of the photons

Published: June 1, 2020

https://dx.doi.org/10.1021/acsnano.0c03704
ACS Nano 2020, 14, 6366–6375

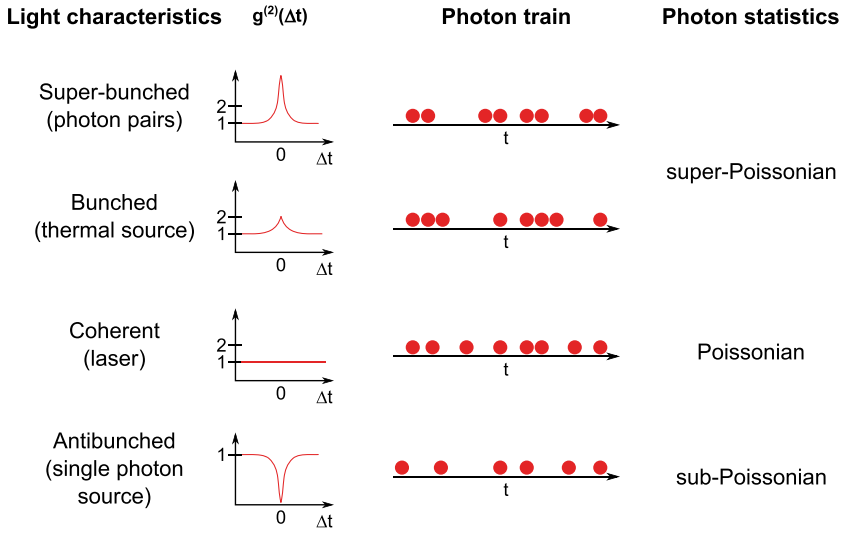

Figure 1. Overview of the light intensity correlation function $g^{(2)}(\Delta t)$ for various light sources. The presented photon trains are cartoons of the photon distributions for the corresponding photon statistics and $g^{(2)}(\Delta t)$.

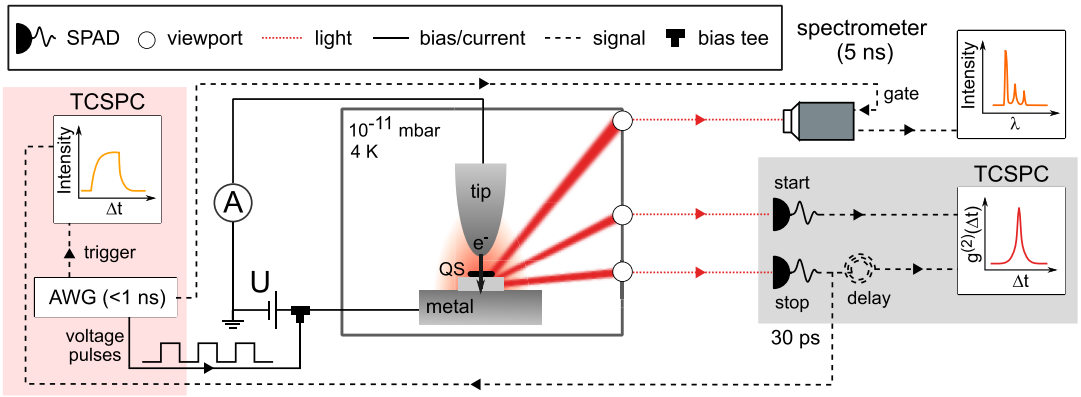

Figure 2. Schematic of a scanning tunneling microscope (STM) combined with a time-resolved optical detection system. The light emitted from the tunnel junction, for example from a quantum state (QS), is collected by three lenses located in the STM head (not shown) and guided through viewports toward detectors located in the ambient (single-photon avalanche photodiodes, SPADs, and a gated optical spectrometer). A time-correlated single-photon counting (TCSPC) module enables time-resolved STML (red shaded box) and Hanbury Brown−Twiss STM (gray shaded box) measurements. AWG, arbitrary wave generator.

within such a beam provides information on the dynamical nature of the light source, which is captured by computing photon time correlations. Mathematically, they are described by the second-order correlation function $g^{(2)}(\Delta t)$ of the electromagnetic field, defined by the time-dependent light intensity $P(t)$:

$$g^{(2)}(\Delta t) = \frac{\langle P(t)P(t+\Delta t)\rangle}{\langle P(t)\rangle\langle P(t+\Delta t)\rangle} \quad (1)$$

where the $g^{(2)}(\Delta t)$ function describes the likelihood to emit a photon at time delay before ($\Delta t < 0$) or after ($\Delta t > 0$) a given emission process that occurred at time t. This function is normalized such that $g^{(2)}(\Delta t \to \pm\infty) = 1$ because the emitter "loses memory" of all previous emission events for long time delays. Typical regimes of $g^{(2)}(\Delta t)$ are shown in Figure 1. In the simplest case, $g^{(2)}(\Delta t)$ is unity for all Δt (third row in Figure 1) if photons are emitted in independent events (Poissonian statistics), as is the case for coherent light (*e.g.*, from a single-mode laser).

Next, let us consider nonunity values of the correlation function for short delay times. The $g^{(2)}(0) > 1$ condition is evidence of photon bunching for classical chaotic light ($1 < g^{(2)}(0) \leq 2$, second row in Figure 1) and superbunching ($g^{(2)}(0) > 2$, top row in Figure 1), which may occur for photon pair emission or an intensity-modulated light source. Finally, there is antibunching ($g^{(2)}(0) < 1$) for which the simultaneous emission of two light quanta is reduced over a time interval $\tau > 0$, which, in turn, can relate to the intrinsic lifetime of the emitting state or its refilling time. In the extreme case of a perfect single-photon emitter, $g^{(2)}(0) = 0$ (bottom row in Figure 1), two photons are never emitted simultaneously. In practice, a source is often designated as a single-photon emitter if an experiment yields $g^{(2)}(0) < 0.5$ because this condition already rules out the existence of two simultaneous emission processes having the same emission rate. Due to the intrinsic time-dependent character, photon correlations are an excellent tool to explore the dynamics of quantum emitters, their associated intrinsic lifetimes, and even mechanisms of bunched emission (*e.g.*, beam chopping).

The experimental setup that we use for a wide variety of STM-based time-resolved studies is schematically presented in Figure 2. The setup comprises a low-temperature (4 K), ultrahigh

https://dx.doi.org/10.1021/acsnano.0c03704
ACS Nano 2020, 14, 6366−6375

vacuum (UHV) STM with three independent free space optical access pathways[11] for time-resolved detection systems situated in the ambient. It is one of a few similar set-ups in the field.[6,12−18] In order to address ultrafast phenomena, the electroluminescence detection is performed by single-photon avalanche photodiodes (SPADs) with 30 ps time resolution (equal to the output pulse jitter with respect to photon arrival) and by an optical spectrometer coupled to an intensifier-gated charge-coupled device (CCD) camera with a minimum gate width of 5 ns. In the following, we distinguish between the Hanbury Brown−Twiss STM (HBT-STM, photon−photon correlation) and time-resolved STML (TR-STML, voltage pulse−photon correlation) modes of operation.

In the HBT-STM intensity interferometer mode (gray box, Figure 2),[5,6,19−22] the time-correlated single-photon counting (TCSPC) PC card measures the distribution of time intervals between registered start and stop photons with a 30 ps (detector-limited) time resolution, which enables determining $g^{(2)}(\Delta t)$ using eq 1. The number of measured correlations per time bin is $N = T\nu_1\nu_2\tau_{ch}$, where T is the integration time, ν_1 and ν_2 are the respective count rates of the two detectors, and τ_{ch} is the width of each time bin. Alternatively, for a configuration with only one SPAD,[23] TCSPC time tagging records the absolute arrival time of each detected photon, enabling a subsequent or on-the-fly calculation of the correlation function (see the Supporting Information for more details). However, in this one-detector configuration, the time-resolution is limited to a few μs, because of after-pulsing artifacts[24] that lead to spurious $g^{(2)}(\Delta t) > 1$ features for $\Delta t < 1$ μs. Ultimately, the SPAD dead time (~100 ns) limits the time resolution of the one-detector approach.

An arbitrary wave generator (AWG) enables one to send tailored[25] voltage pulses to the tunnel junction with a time resolution of approximately 1 ns, which is a limitation that results from the wires connected to the STM junction.[25,26] The TR-STML technique (pink box, Figure 2) registers the time evolution of electroluminescence ($P(\Delta t)$, yellow trace in Figure 2) upon application of a rectangular voltage pulse. It is used to perform experiments for which a time resolution of 1 ns is sufficient. In contrast to HBT-STM, the events per time slot scale linearly with the detector count rate, and, due to triggering by synchronization pulses with a high repetition rate (~1 MHz) compared to typical photon count rate (10−100 kHz), the signal-to-noise ratio is significantly increased in TR-STML.

These different setups discussed above show how dynamical studies of quantum systems with discrete levels can be performed with relative ease at the atomic scale. In all cases, the method profits from the strong local field enhancement present in tip−surface nanocavities.[27] Concurrently, the picometer precise current injection by a STM tip enables studies of entities far smaller than the diffraction limit, such as the luminescence of a single molecule at the subnanometer scale.[28,29] In general, there are two principal emission mechanisms of STML: plasmonic and excitonic. In plasmonic emission, an inelastic electron tunneling process excites nanocavity plasmon modes that may couple to far-field photons with a broadband spectrum ($\Delta E > 100$ meV). In excitonic emission, luminescence occurs due to electron−hole recombination in a decoupled system. Sufficient decoupling can be achieved by separating the emitting system from the metallic electrodes, prominently the substrate, with a thin ($d \approx 0.5$ nm) insulating film, such that the nonradiative decay of the excitation *via* coupling to the metal is strongly reduced, while tunneling is still sufficiently efficient.[29] Under these conditions, the emission spectrum can exhibit spectrally sharp features ($\Delta E < 20$ meV), which can be used to identify the emitter, by comparison with, for example, photoluminescence measurements.[28,30−32]

> The picometer precise current injection by a scanning tunneling microscope tip enables studies of entities far smaller than the diffraction limit, such as the luminescence of a single molecule at the subnanometer scale.

We will next focus on examples of atomic-scale processes that lead to photon bunching and antibunching. We will discuss how to model their dynamics using rate equations, an approach commonly used for analyzing optical processes in quantum optics, such as spontaneous or stimulated emission or photo- or electron-induced luminescence, including single-photon emission.[27]

CLASSICAL PHOTON CORRELATIONS AT THE ATOMIC SCALE

We will start with a simple model system: a telegraphic emitter (Figure 3). It switches randomly between an "on" and an "off" state, thus providing data that resemble historic telegraphic

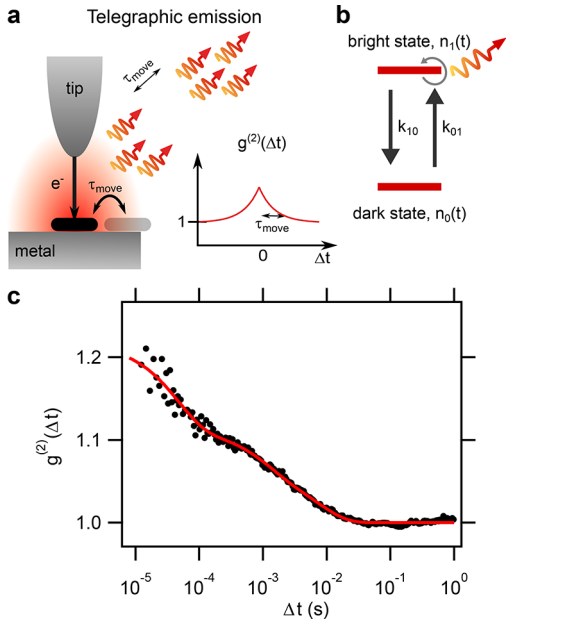

Figure 3. Telegraphic modulation of scanning tunneling microscopy-induced luminescence. (a) Schematic of plasmonic luminescence intensity modulation due to adsorbate motion below the tip. The red shading symbolizes the tip-induced plasmon. Bottom-right: Schematic correlation function $g^{(2)}(\Delta t)$ showing photon bunching over a characteristic time $\tau_{move} = (k_{01} + k_{10})^{-1}$. (b) Two level system consisting of a bright (continuously emitting with a rate k_{11}, gray rounded arrow) and a dark state that the system transitions between, with rates k_{01} and k_{10}. (c) Measured photon bunching $g^{(2)}(\Delta t)$ (black circles) fitted by a triple-exponential function (red line) yielding characteristic time constants of 8 ms, 1 ms, and 45 μs. The slowest time constant τ_{move} = 8 ms is assigned to the lateral diffusion of a single hydrogen molecule below the scanning tunneling microscope tip.[23]

https://dx.doi.org/10.1021/acsnano.0c03704
ACS Nano 2020, 14, 6366−6375

signals. Such systems are often encountered in molecular physics as a result of molecular motion or an oscillating chemical reaction.[33−35] A telegraphic light emitter exhibits classical (intensity-based) photon bunching, as illustrated in Figure 3, by switching between a bright "on" and a dark "off" state with time-dependent populations $n_1(t)$ and $n_0(t)$, respectively. The transition rates k_{10} and k_{01} describe the probabilities of switching between the two states, thus determining the time evolution of the system according to the following Master equation:

$$\frac{d}{dt}\begin{bmatrix} n_0 \\ n_1 \end{bmatrix} = \begin{bmatrix} -k_{01} & k_{10} \\ k_{01} & -k_{10} \end{bmatrix}\begin{bmatrix} n_0 \\ n_1 \end{bmatrix} \tag{2}$$

For initial populations $n_0(0) = 0$, $n_1(0) = 1$ (that is assuming an emission event at $t = 0$):

$$n_1(t) = \frac{1}{k_{01} + k_{10}}(k_{01} + k_{10}e^{-(k_{01}+k_{10})t}) \tag{3}$$

We define the light intensity to be $P(t) = \eta k_{11} n_1(t)$ for a continuous emission from a bright state, where η is the detection efficiency and k_{11} is the emission rate in the bright state. Then, we obtain the following correlation function characterizing the luminescence fluctuations:

$$g^{(2)}(\Delta t) = \frac{P(\Delta t)}{P(\Delta t \to \infty)} = 1 + \frac{k_{10}}{k_{01}}e^{-(k_{01}+k_{10})\Delta t} \tag{4}$$

The characteristic time of the dynamics is $\tau_{move} = (k_{01} + k_{10})^{-1}$. Because $g^{(2)}(0) = 1 + k_{10}/k_{01}$, the photons are bunched and both rates can be extracted from a fit to the measured correlation function. A detailed discussion on this topic can be found elsewhere.[36]

Photon correlations that arise from luminescence fluctuations in time are a perfect means to infer the dynamics of an adsorbate. Importantly, this approach does not require intrinsic emission from the adsorbate but only from inelastic tunneling (plasmonic emission), an easily achieved condition, which enables studies on a broad range of systems. The phenomena can be tracked with picosecond resolution, greatly extending the temporal range of tunneling current correlations in STM (typically limited to ~0.1 ms). The first studies employing this approach focused on a qualitative description of the nanoscale dynamics of adsorbates.[19−21] We have used the same approach to quantify the dynamics of a single H_2 molecule within a well-defined low-coverage Fermi lattice on Au(111).[23] An example of photon bunching for that system in the millisecond to microsecond regime is shown in Figure 3c. The motion of the molecules in the STM junction modifies the intensity of the plasmonic luminescence creating bunches of photons. As demonstrated recently, photon correlations can be used to track the dynamics of single-molecule tautomerization.[37] We envision further studies on the dynamics of molecular devices such as motors[38,39] and related diffusive and catalytic processes at the single-atom level.[40,41]

QUANTUM EMITTERS

The next important class of systems is formed by quantum emitters that produce photons linked with each other by quantum mechanical relations originating at the atomic scale. Single photon or photon pair sources belong to this category and are one of the most promising routes for the implementation of quantum computing and cryptography. The simplest description of a single-photon emitter requires only two states (ground and excited states). A single photon is emitted upon transition from an excited to a ground state, as realized in the photoluminescence of a single molecule or quantum dot. The emitting state is excited with a rate k_{01} and decays with a rate k_{10} (Figure 4b). Solving eq 2 (with initial conditions $n_0(0) = 1$, $n_1(0) = 0$, that is, assuming an emission event at $t = 0$) yields

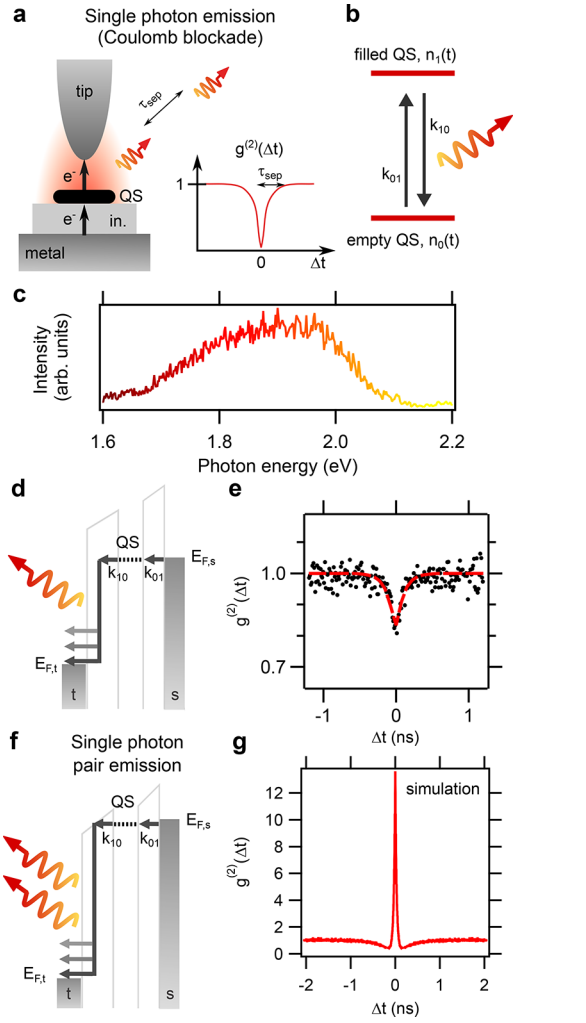

Figure 4. Plasmonic single-photon emission from an isolated quantum state (QS). (a) Schematic for a single-photon emitter based on the Coulomb blockade of electron tunneling. Vacuum gap and insulating layer (in.) decouple the QS from the electrodes on both sides (tip and metal sample). Individual electrons tunnel at intervals $\tau_{sep} = (k_{01} + k_{10})^{-1}$ and impose an anticorrelation on the spectrally broad plasmonic emission as shown in (c), here on Au(111), $U = -3$ V, $I = 100$ pA. Bottom right: Schematic $g^{(2)}(\Delta t)$ function showing photon antibunching with a recovery time τ_{sep}. (d) Energy scheme of the emitter with QS refilling rate k_{01} and tunnel rate k_{10}. During electron tunneling, plasmons can be excited leading to photon emission. (e) Example of Coulomb blockade-induced plasmonic antibunching from a tip-induced quantum dot on a defect-free area of a C_{60} molecular film, indicating imperfect single-photon emission.[42] $U = -3.67$ V, $I = 2$ nA. (f) Energy scheme for a suggested single-photon-pair emission process. Unlike case (d), a photon pair is emitted during a single inelastic tunneling event. (g) The simulated correlation $g^{(2)}(\Delta t)$ for this process exhibits a central bunching peak due to photon pair generation and antibunching wings due to Coulomb-blockaded electron tunneling. Further details can be found in the Supporting Information.

https://dx.doi.org/10.1021/acsnano.0c03704
ACS Nano 2020, 14, 6366−6375

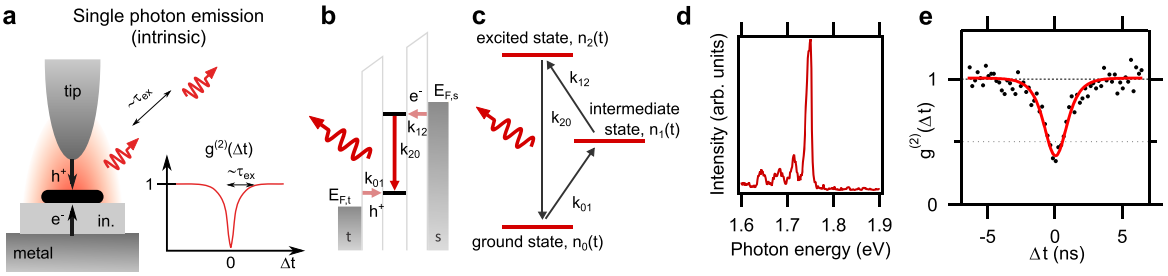

Figure 5. Excitonic scanning tunneling microscopy-induced luminescence from an individual system. (a) Schematic of a single-photon emitter with intrinsic exciton recombination. Bottom right: Schematic $g^{(2)}(\Delta t)$ function showing photon antibunching with a statistical recovery time τ_{ex}, which indicates the minimum separation between successive photons. (b) Energy scheme of a system emitting during recombination with time constant k_{20} following hole and electron injection with rate constants k_{01} and k_{12}, respectively. The process requires the bias voltage to shift both the electron and the hole levels of the system into the energy window between the tip and sample Fermi energies (E_F). (c) Three-state diagram of the same dynamic system. (d) Typical excitonic spectrum of an emission center in a C_{60} thin film with a strong electronic transition and vibrational progressions toward lower photon energies, $U = -3$ V, $I = 100$ pA. (e) Hanbury Brown−Twiss scanning tunneling microscopy measurement of excitonic antibunched electroluminescence from a C_{60} emission center, $U = -3.2$ V, $I = 50$ pA, for which the recovery time is dominated by the exciton lifetime ($\tau_{ex} \approx 1/k_{20}$). The red line is a fit to the data with $\tau_{ex} = 733$ ps convoluted with the detector response function.

$$n_1(t) = \frac{1}{k_{01} + k_{10}}(k_{01} - k_{01}e^{-(k_{01}+k_{10})t}) \tag{5}$$

The light intensity is

$$P(t) = \eta k_{10} n_1(t) \tag{6}$$

and the correlation function is

$$g^{(2)}(\Delta t) = \frac{P(\Delta t)}{P(\Delta t \to \infty)} = 1 - e^{-(k_{01}+k_{10})\Delta t} \tag{7}$$

which becomes 0 for $\Delta t = 0$, demonstrating perfect antibunched emission.

In addition to molecules or quantum dots, single-photon emitters can be realized by exploiting a Coulomb blockade (Figure 4a).[42] This effect is operative for a wide range of bias voltages and relies on tunneling through an electronic quantum state (QS), which can be occupied by only one electron at a time due to Coulomb repulsion. As a result, electrons flow one-by-one, in an antibunched manner, exciting the tip-induced plasmon (Figure 4c) *via* the inelastic tunneling process (Figure 4d,e) in a temporally antibunched way. When an individual tunneling event can only produce a single photon, this 1:1 relationship also ensures that the light emission that is plasmonic in nature can behave as a single-photon emitter. The Coulomb blockaded single-photon emitter may be used as a basis for constructing more sophisticated quantum light sources. Because single electron tunneling under specific conditions can emit more than one photon,[22,43] one may expect to observe single pair emission (Figure 4f,g), that is, each pair emission event is embedded in a time interval free of any other photon. In the future, such concepts could be applied, for instance, in optoelectronic devices based on inelastic tunneling.[44−47]

So far, we have used a two-state kinetic model to analyze time-resolved plasmonic electroluminescence. Spectrally sharp intrinsic excitonic emission (Figure 5d) can also be described in this framework if the system is excited with incoming light or by a locally excited plasmon in the junction. However, exciton generation with direct charge injection requires at least a three-state kinetic model description.[5,26,48] An example is given in Figure 5b, where first the hole is created on the molecule or defect by extracting an electron with a rate k_{01}, followed by the injection of an electron into a higher level with a rate k_{12}. This sequence can also occur in reverse order. When both processes have occurred, an electron−hole pair (exciton) forms. Finally, this exciton decays with a rate k_{20}, which can lead to light emission (radiative decay). The sequence is summarized in a diagram (Figure 5c) whose parameters satisfy:

$$\frac{d}{dt}\begin{bmatrix} n_0 \\ n_1 \\ n_2 \end{bmatrix} = \begin{bmatrix} -k_{01} & 0 & k_{20} \\ k_{01} & -k_{12} & 0 \\ 0 & k_{12} & -k_{20} \end{bmatrix}\begin{bmatrix} n_0 \\ n_1 \\ n_2 \end{bmatrix} \tag{8}$$

Following the same approach as for the Coulomb blockade case, we obtain

$$g^{(2)}(\Delta t) = 1 + \frac{S - Q}{2Q}e^{-S+Q/2\Delta t} - \frac{S + Q}{2Q}e^{-S-Q/2\Delta t} \tag{9}$$

with $S = k_{01} + k_{12} + k_{20}$ and $Q = (S^2 - 4(k_{01}k_{12} + k_{12}k_{20} + k_{20}k_{01}))^{0.5}$. Here, $g^{(2)}(0) = 0$, thus, the system is an electrically driven single-photon emitter. The width of the dip observed in correlation measurements in this case is modulated by two exponential functions in eq 9, which results in a broader parabolic rise of the antibunching dip compared to the linear single exponential rise that is observed for the same emitter if the excitation took place by photon absorption (photoluminescence).[49]

Single-photon emission from individual defects[5] or molecules[6] reported by STML (Figure 5a) is described well by three-state models. Considering typical HBT-STM thin-film conditions (slow k_{01}, fast k_{12}),[5,6] the recovery time of the measured dip in $g^{(2)}(\Delta t)$ is usually dominated by the exciton lifetime τ_{ex}. We note that in eqs 8 and 9 the three time constants of the model may be permuted without changing the resulting correlation function. Thus, additional arguments that are separate from the model are required in order to assign the model rate constants to specific physical processes. If, for instance, a high Purcell factor reduces the exciton lifetime drastically, the charge transfer to, or from, the substrate may be dominating the measured correlation, albeit the tunneling current toward the tip remains low.

In addition to probing single photon emitters with atomic precision, scanning tunneling microscopy enables their lifetime manipulation. In Figure 5e we present an emission center in a thin C_{60} film, the first single-photon emitter explored by STML.[5] The exciton lifetime can be increased by improving the

https://dx.doi.org/10.1021/acsnano.0c03704
ACS Nano 2020, 14, 6366−6375

decoupling from the metal substrate[6] or decreased by applying higher tunneling current.[5] Although an equivalent behavior in optically pumped quantum dots is usually attributed to exciton−exciton annihilation,[50] here, the dominance of charge carriers suggests that an entirely different mechanism is at work, which involves the tuning of nonradiative decay through charge−exciton annihilation.[5] This mechanism enables using the charge injection *via* tunneling current as an "internal clock", permitting one to monitor the picosecond dynamics of a single-photon emitter simply by investigating its emission efficiency as a function of tunneling current.[5,26,51] The $P(\tau_{\text{tunnel}})$ dependency (equivalent to $P(I/e)$) can be obtained by calculating $P(t \to \infty)$ and then introducing charge−exciton annihilation as an additional quenching channel.[51] However, the mechanism may not be generalizable; it was reported that $P(I)$ can also increase in a superlinear way for moderate tunneling currents, an effect that is attributed to an increase in the radiative rate with respect to the nonradiative decay.[6,52]

> In addition to probing single photon emitters with atomic precision, scanning tunneling microscopy enables their lifetime manipulation.

Processes slower than exciton decay, like charge injection, can be more readily addressed using TR-STML. In this approach, a train of nanosecond voltage pulses drives the system periodically out of equilibrium and the transient light response is monitored and accumulated over millions of pulse repetitions. This standard transient electroluminescence technique, which is normally used in organic optoelectronics,[53,54] can now be implemented in STML, resulting in a methodology capable of spatially resolved scanning over an individual emitter, which opens new research avenues on the relation between molecular electronic structure and optical properties.[26]

MODELING COMPLEX SYSTEMS NUMERICALLY

Although the analytical description presented above captures the peculiarities of simple emitters, many imaginable light-emitting systems and stochastic process networks are too complicated to have their dynamics treated analytically. Nevertheless, it has proven useful to simulate their behavior in combination with the performance of the photon detection and correlation hardware, which enables a quick assessment and exploration of features observed in correlation data. For this purpose, we use the Monte Carlo approach to simulate the evolution of a multistate system with rate-governed transitions between its states. We generate a random sequence of processes through which the system moves from state to state, which is based on *ad-hoc*-generated (pseudo) random numbers. If defined as radiative, a transition can result in a signal in an emulated detector. The final output of the simulation is the time correlation function after the system has undergone thousands to millions of transitions (see the Supporting Information for more details). Monte Carlo simulations make it possible to model correlation measurements (HBT-STM) or the evolution of a system driven by periodic voltage (TR-STML) or laser pulses in a simple manner. In this Perspective, we employ such simulations to predict the behavior of a single-pair emitter (Figure 4g), a combined singlet−triplet emitter (Figure 6c), and exciton−plasmon cross-correlations (Figure 7b), all of which are eagerly anticipated developments in the field.

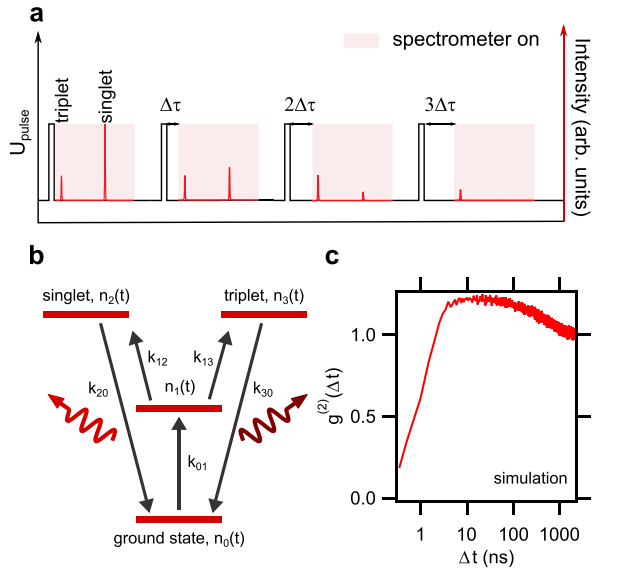

Figure 6. Triplet emission time-resolved spectroscopy simulations. (a) Principle of a gated spectroscopy experiment. The decay of the singlet and triplet state (lifetimes of the ns and μs scale, respectively) is measured by applying a voltage pulse exciting the system and providing the trigger to open the spectrometer gate after a varied delay time Δτ. (b) Four-state model of a singlet−triplet emitter. The system is driven to the intermediate charged state from which a singlet or a triplet state is formed that depends on the spin of the injected charges relative to the spin already present. (c) Simulation of $g^{(2)}(\Delta t)$ (see main text) for the system presented in (b). The antibunching is due to the presence of one excited state at a time, and the bunching in the μs regime is due to the presence of a triplet shelving state. Simulation details can be found in the Supporting Information.

FUTURE DIRECTIONS OF THE FIELD

The time evolution of the optical emission spectra after initial excitation can be monitored with gated optical spectroscopy. This method is particularly well suited for investigating singlet and triplet dynamics, because their time scales are very different. Fluorescence lifetimes (singlet decay) are usually on the order of a few nanoseconds, while phosphorescence lifetimes (triplet decay) can be as long as a few microseconds. State-of-the-art intensified CCD detectors have the requisite few nanosecond gate length and gate delay time scales for such a measurement. Gated measurements may be able to clarify how local energy transfer happens, such as the intersystem-crossing dynamics of room-temperature organic phosphors.[55] A sequence of short voltage pulses (Figure 6a) from an AWG is used to excite the quantum system. By synchronizing the pulses with the gating of the CCD intensifier and varying the gate delay, one can obtain the transient spectral response before, during, and after the voltage pulse.

Recently, the existence of bright[56] and dark[57] triplet states in molecules was reported in STML. A triplet state might manifest itself in HBT-STM measurements from a single molecule because it acts as a shelving state for singlet emission, resulting in singlet emission at short and long time scales that is antibunched and bunched, respectively (Figure 6c). The time constant of the bunching decay can be directly linked to the characteristic spin-

https://dx.doi.org/10.1021/acsnano.0c03704
ACS Nano 2020, 14, 6366−6375

triplet state lifetime. Moreover, electroluminescence, unlike photoluminescence, enables not only charge-induced annihilation but also up-conversion of a triplet excitonic state to the singlet state.[57] We expect that these detailed processes and their relative weights and conditions will be explored in the near future.

Extended information on the dynamics of quantum systems can be gained by measuring photon time cross-correlations between different emission channels. A measurement on the bimodal excitonic−plasmonic emission from C_{60} defects,[51] for example, can be realized by spectral filtering the excitonic line for one time-resolved detector and blocking this same line (*i.e.*, admitting only the plasmonic component) for the second detector. Such a measurement can access the temporal sequence of both emission mechanisms and how they are linked within the internal dynamics of the system. Because each electron injected from the substrate can transfer its energy for either exciton or plasmon formation, we may speculate on finding a complex cross-antibunched correlation that can elucidate several time constants of the system at once (Figure 7b). A similar shape of the correlation function has been reported for the cross-correlation of the biexciton−exciton emission cascade in quantum dots.[58]

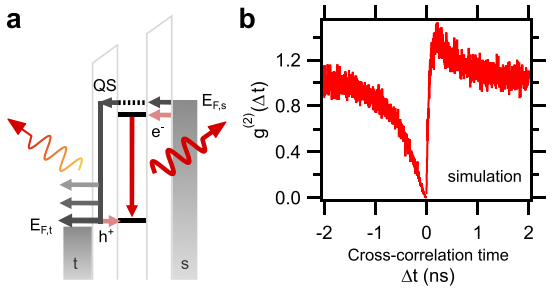

Figure 7. Bimodal excitonic-plasmonic scanning tunneling microscopy-induced luminescence. (a) Energy scheme of a source showing both excitonic (red arrow) and plasmonic (multicolored arrow) emission. Photons can be created either by an inelastic tunneling path (plasmonic) or the intrinsic decay of an exciton. (b) Simulated cross-correlation between the two emission channels of the bimodal emitter (for details see main text and Supporting Information).

The application of cross-correlations may be extended to a variety of systems. Recently, it has been shown that quantum emitters like individual phthalocyanines can be optically excited locally with tip-induced plasmons.[59−61] When excitons and plasmons interact in the strong coupling regime,[62] Rabi oscillations, which are evidence of the mixed light−matter state, may be observable with HBT-STM.[63] Similarly, correlations between different excitonic channels may be employed to explore quantum systems. Because a molecular emitter can have excitons at different energies, those may interact with one another, leading to energy upconversion or mutual annihilation. Moreover, a single high-energy exciton may decay into two lower energy excitons, a process known as exciton fission,[64] which is highly sought after in solar energy conversion. Combining the techniques outlined in this Perspective may address the order of the conversion transition, the role of intermediate charge injection, time constants, and spectral relations. In general, studies of interacting molecular systems may one day enable researchers to tailor dynamic systems that produce elaborate photon emission sequences. Similarly, we envision the realization of photon-on-demand sources based on a pump−probe scheme[65] using TR-STML, where each of the two pulses would inject one of the required complementary charges.[48]

Moreover, we expect that future studies will focus on *in situ* assembled aggregates in order to study collective effects with atomic precision. When molecular quantum emitters are brought close to each other, they start to exchange energy through incoherent[16] or coherent[66] interactions, which eventually form a single coupled system[67] and potentially emit entangled photons.[68] One molecular emitter may also be a source of single photons that interact with another molecule.[69] A different topic of interest is the atomic-scale origin of single-photon emitters in two-dimensional materials.[70−75] Here, intrinsic or extrinsic defects will play the crucial role, similar to the excitonic emission from defects in thin C_{60} films described earlier. In the next step, the interaction between defects and individual luminescent molecules[76] could be investigated as it enables various three-dimensional arrangements between the transition dipoles of the emitters. Finally, in-plane distance dependencies on the atomic scale may be addressed by defining two distinct positions on an otherwise homogeneous film, one position given by a luminescent defect and the second by the position of charge injection from the STM tip. In this way, it is possible to map variations of dynamic constants laterally to investigate the tuning of charge injection rates.[77] Such studies may be further refined to include the electric-field contributions and the tip-induced enhancement effects, both of which are strongly related to the atomic structure of the tip apex, defining the so-called picocavity.[78]

> We expect that future studies will focus on *in situ* assembled aggregates in order to study collective effects with atomic precision.

In conclusion, picosecond photon correlations combined with STML are a powerful tool to study the finest details of light−matter interactions and dynamics of single entities at the atomic scale. This approach enables probing the motion of molecules as small as hydrogen, the dynamics of individual electrons, holes, and excitons, as well as the interactions between excitons and plasmons. Quantum properties of light are directly accessed with the spatial precision of STM, which provides experimentalists with exquisite control over individual single photon or photon pair emitters, all of which is necessary for future quantum information processing technologies.

Improving the time resolution can further extend the possibilities enabled by combining STM with time-resolved luminescence. Currently, photon−photon correlation measurements are limited by the output pulse time jitter of the employed SPAD detector (*ca.* 30 ps). However, schemes with much better temporal resolution and sufficient efficiency, such as elaborate streak cameras, have been commercialized. Moreover, by means of single-photon up-conversion with femtosecond pump pulses, single photons have been detected with 25% efficiency with a time resolution of 150 fs.[79] Recently, even higher efficiencies have been reported.[80] Note, however, that these efficiencies apply only within the time overlap of single photons with the femtosecond pump pulse. To obtain the efficiency for photons continuously generated (*e.g.*, in the STM), the duty cycle of the up-conversion pulses has to be taken into consideration. Another approach toward faster time scales could be based on

https://dx.doi.org/10.1021/acsnano.0c03704
ACS Nano 2020, 14, 6366−6375

two-photon interference detected in the Hong−Ou−Mandel scheme,[81] which may enable researchers to measure the photon wave packet with attosecond resolution.[82] From these trends, we believe that the ground is fertile for future research to bring together the best of spatial and temporal resolution techniques.

ASSOCIATED CONTENT

Supporting Information

The Supporting Information is available free of charge at https://pubs.acs.org/doi/10.1021/acsnano.0c03704.

Computation of $g^{(2)}(\Delta t)$, Monte Carlo simulations of systems described by rate equations, single photon pair emission correlation simulation, singlet−triplet emission correlation simulation, exciton−plasmon correlation simulation (PDF)

AUTHOR INFORMATION

Corresponding Authors

Anna Rosławska − *Max-Planck-Institut für Festkörperforschung, 70569 Stuttgart, Germany;* orcid.org/0000-0002-0317-1775; Email: roslawska@ipcms.unistra.fr

Klaus Kuhnke − *Max-Planck-Institut für Festkörperforschung, 70569 Stuttgart, Germany;* orcid.org/0000-0001-9981-1732; Email: k.kuhnke@fkf.mpg.de

Authors

Christopher C. Leon − *Max-Planck-Institut für Festkörperforschung, 70569 Stuttgart, Germany;* orcid.org/0000-0003-4132-4645

Abhishek Grewal − *Max-Planck-Institut für Festkörperforschung, 70569 Stuttgart, Germany*

Pablo Merino − *Max-Planck-Institut für Festkörperforschung, 70569 Stuttgart, Germany; Instituto de Ciencia de Materiales de Madrid, CSIC, E28049 Madrid, Spain; Instituto de Física Fundamental, CSIC, E28006 Madrid, Spain;* orcid.org/0000-0002-0267-4020

Klaus Kern − *Max-Planck-Institut für Festkörperforschung, 70569 Stuttgart, Germany; Institut de Physique, École Polytechnique Fédérale de Lausanne, 1015 Lausanne, Switzerland*

Complete contact information is available at: https://pubs.acs.org/10.1021/acsnano.0c03704

Author Contributions

‡These authors contributed equally.

Funding

P.M. acknowledges the A. v. Humboldt Stiftung for their support.

Notes

The authors declare no competing financial interest.

ACKNOWLEDGMENTS

We would like to thank G. Schull, D. G. de Oteyza, and O. Gunnarsson for fruitful discussions.

REFERENCES

(1) Krausz, F.; Ivanov, M. Attosecond Physics. *Rev. Mod. Phys.* **2009**, *81*, 163−234.

(2) Garg, M.; Zhan, M.; Luu, T. T.; Lakhotia, H.; Klostermann, T.; Guggenmos, A.; Goulielmakis, E. Multi-Petahertz Electronic Metrology. *Nature* **2016**, *538*, 359−363.

(3) Bücker, K.; Picher, M.; Crégut, O.; LaGrange, T.; Reed, B. W.; Park, S. T.; Masiel, D. J.; Banhart, F. Electron Beam Dynamics in an Ultrafast Transmission Electron Microscope with Wehnelt Electrode. *Ultramicroscopy* **2016**, *171*, 8−18.

(4) Rubiano da Silva, N.; Möller, M.; Feist, A.; Ulrichs, H.; Ropers, C.; Schäfer, S. Nanoscale Mapping of Ultrafast Magnetization Dynamics with Femtosecond Lorentz Microscopy. *Phys. Rev. X* **2018**, *8*, 031052.

(5) Merino, P.; Große, C.; Rosławska, A.; Kuhnke, K.; Kern, K. Exciton Dynamics of C_{60}-Based Single-Photon Emitters Explored by Hanbury Brown−Twiss Scanning Tunnelling Microscopy. *Nat. Commun.* **2015**, *6*, 8461.

(6) Zhang, L.; Yu, Y.-J.; Chen, L.-G.; Luo, Y.; Yang, B.; Kong, F.-F.; Chen, G.; Zhang, Y.; Zhang, Q.; Luo, Y.; Yang, J.-L.; Dong, Z.-C.; Hou, J. G. Electrically Driven Single-Photon Emission from an Isolated Single Molecule. *Nat. Commun.* **2017**, *8*, 580.

(7) Cocker, T. L.; Peller, D.; Yu, P.; Repp, J.; Huber, R. Tracking the Ultrafast Motion of a Single Molecule by Femtosecond Orbital Imaging. *Nature* **2016**, *539*, 263−267.

(8) Terada, Y.; Yoshida, S.; Takeuchi, O.; Shigekawa, H. Real-Space Imaging of Transient Carrier Dynamics by Nanoscale Pump-Probe Microscopy. *Nat. Photonics* **2010**, *4*, 869−874.

(9) Kloth, P.; Wenderoth, M. From Time-Resolved Atomic-Scale Imaging of Individual Donors to their Cooperative Dynamics. *Sci. Adv.* **2017**, *3*, No. e1601552.

(10) Garg, M.; Kern, K. Attosecond Coherent Manipulation of Electrons in Tunneling Microscopy. *Science* **2020**, *367*, 411−415.

(11) Kuhnke, K.; Kabakchiev, A.; Stiepany, W.; Zinser, F.; Vogelgesang, R.; Kern, K. Versatile Optical Access to the Tunnel Gap in a Low-Temperature Scanning Tunneling Microscope. *Rev. Sci. Instrum.* **2010**, *81*, 113102.

(12) Edelmann, K.; Gerhard, L.; Winkler, M.; Wilmes, L.; Rai, V.; Schumann, M.; Kern, C.; Meyer, M.; Wegener, M.; Wulfhekel, W. Light Collection from a Low-Temperature Scanning Tunneling Microscope Using Integrated Mirror Tips Fabricated by Direct Laser Writing. *Rev. Sci. Instrum.* **2018**, *89*, 123107.

(13) Sheng, S.; Li, W.; Gou, J.; Cheng, P.; Chen, L.; Wu, K. Low-Temperature, Ultrahigh-Vacuum Tip-Enhanced Raman Spectroscopy Combined with Molecular Beam Epitaxy for *in Situ* Two-Dimensional Materials' Studies. *Rev. Sci. Instrum.* **2018**, *89*, 053107.

(14) Wu, Z.-B.; Gao, Z.-Y.; Chen, X.-Y.; Xing, Y.-Q.; Yang, H.; Li, G.; Ma, R.; Wang, A.; Yan, J.; Shen, C.; Du, S.; Huan, Q.; Gao, H. J. A Low-Temperature Scanning Probe Microscopy System with Molecular Beam Epitaxy and Optical Access. *Rev. Sci. Instrum.* **2018**, *89*, 113705.

(15) Reecht, G.; Scheurer, F.; Speisser, V.; Dappe, Y. J.; Mathevet, F.; Schull, G. Electroluminescence of a Polythiophene Molecular Wire Suspended between a Metallic Surface and the Tip of a Scanning Tunneling Microscope. *Phys. Rev. Lett.* **2014**, *112*, 047403.

(16) Imada, H.; Miwa, K.; Imai-Imada, M.; Kawahara, S.; Kimura, K.; Kim, Y. Real-Space Investigation of Energy Transfer in Heterogeneous Molecular Dimers. *Nature* **2016**, *538*, 364−367.

(17) Hoffmann, G.; Kröger, J.; Berndt, R. Color Imaging with a Low Temperature Scanning Tunneling Microscope. *Rev. Sci. Instrum.* **2002**, *73*, 305−309.

(18) Böckmann, H.; Liu, S.; Müller, M.; Hammud, A.; Wolf, M.; Kumagai, T. Near-Field Manipulation in a Scanning Tunneling Microscope Junction with Plasmonic Fabry-Pérot Tips. *Nano Lett.* **2019**, *19*, 3597−3602.

(19) Silly, F.; Charra, F. Time-Autocorrelation in Scanning-Tunneling-Microscope-Induced Photon Emission from Metallic Surface. *Appl. Phys. Lett.* **2000**, *77*, 3648−3650.

(20) Silly, F.; Charra, F. Time-Correlations as a Contrast Mechanism in Scanning-Tunneling-Microscopy-Induced Photon Emission. *Ultramicroscopy* **2004**, *99*, 159−164.

(21) Perronet, K.; Schull, G.; Raimond, P.; Charra, F. Single-Molecule Fluctuations in a Tunnel Junction: A Study by Scanning-Tunnelling-Microscopy-Induced Luminescence. *EPL Europhys. Lett.* **2006**, *74*, 313.

(22) Leon, C. C.; Rosławska, A.; Grewal, A.; Gunnarsson, O.; Kuhnke, K.; Kern, K. Photon Superbunching from a Generic Tunnel Junction. *Sci. Adv.* **2019**, *5*, No. eaav4986.

(23) Merino, P.; Rosławska, A.; Leon, C. C.; Grewal, A.; Große, C.; González, C.; Kuhnke, K.; Kern, K. A Single Hydrogen Molecule as an Intensity Chopper in an Electrically Driven Plasmonic Nanocavity. *Nano Lett.* **2019**, *19*, 235−241.
(24) Becker, W. *The bh TCSPC Handbook*, 6th ed.; Becker & Hickl GmbH: Berlin, Germany, 2014.
(25) Grosse, C.; Etzkorn, M.; Kuhnke, K.; Loth, S.; Kern, K. Quantitative Mapping of Fast Voltage Pulses in Tunnel Junctions by Plasmonic Luminescence. *Appl. Phys. Lett.* **2013**, *103*, 183108.
(26) Rosławska, A.; Merino, P.; Große, C.; Leon, C. C.; Gunnarsson, O.; Etzkorn, M.; Kuhnke, K.; Kern, K. Single Charge and Exciton Dynamics Probed by Molecular-Scale-Induced Electroluminescence. *Nano Lett.* **2018**, *18*, 4001−4007.
(27) Novotny, L.; Hecht, B. *Principles of Nano-Optics*; Cambridge University Press: Cambridge, UK, 2012.
(28) Qiu, X. H.; Nazin, G. V.; Ho, W. Vibrationally Resolved Fluorescence Excited with Submolecular Precision. *Science* **2003**, *299*, 542−546.
(29) Kuhnke, K.; Große, C.; Merino, P.; Kern, K. Atomic-Scale Imaging and Spectroscopy of Electroluminescence at Molecular Interfaces. *Chem. Rev.* **2017**, *117*, 5174−5222.
(30) Dong, Z.-C.; Guo, X.-L.; Trifonov, A. S.; Dorozhkin, P. S.; Miki, K.; Kimura, K.; Yokoyama, S.; Mashiko, S. Vibrationally Resolved Fluorescence from Organic Molecules near Metal Surfaces in a Scanning Tunneling Microscope. *Phys. Rev. Lett.* **2004**, *92*, 086801.
(31) Doppagne, B.; Chong, M. C.; Lorchat, E.; Berciaud, S.; Romeo, M.; Bulou, H.; Boeglin, A.; Scheurer, F.; Schull, G. Vibronic Spectroscopy with Submolecular Resolution from STM-Induced Electroluminescence. *Phys. Rev. Lett.* **2017**, *118*, 127401.
(32) Große, C.; Merino, P.; Rosławska, A.; Gunnarsson, O.; Kuhnke, K.; Kern, K. Submolecular Electroluminescence Mapping of Organic Semiconductors. *ACS Nano* **2017**, *11*, 1230−1237.
(33) Liljeroth, P.; Repp, J.; Meyer, G. Current-Induced Hydrogen Tautomerization and Conductance Switching of Naphthalocyanine Molecules. *Science* **2007**, *317*, 1203−1206.
(34) Aragonès, A. C.; Haworth, N. L.; Darwish, N.; Ciampi, S.; Bloomfield, N. J.; Wallace, G. G.; Diez-Perez, I.; Coote, M. L. Electrostatic Catalysis of a Diels-Alder Reaction. *Nature* **2016**, *531*, 88−91.
(35) Kumagai, T.; Hanke, F.; Gawinkowski, S.; Sharp, J.; Kotsis, K.; Waluk, J.; Persson, M.; Grill, L. Controlling Intramolecular Hydrogen Transfer in a Porphycene Molecule with Single Atoms or Molecules Located Nearby. *Nat. Chem.* **2014**, *6*, 41−46.
(36) Lippitz, M.; Kulzer, F.; Orrit, M. Statistical Evaluation of Single Nano-Object Fluorescence. *ChemPhysChem* **2005**, *6*, 770−789.
(37) Doppagne, B.; Neuman, T.; Soria-Martinez, R.; López, L. E. P.; Bulou, H.; Romeo, M.; Berciaud, S.; Scheurer, F.; Aizpurua, J.; Schull, G. Single-Molecule Tautomerization Tracking through Space- and Time-Resolved Fluorescence Spectroscopy. *Nat. Nanotechnol.* **2020**, *15*, 207−211.
(38) Tierney, H. L.; Murphy, C. J.; Jewell, A. D.; Baber, A. E.; Iski, E. V.; Khodaverdian, H. Y.; McGuire, A. F.; Klebanov, N.; Sykes, E. C. H. Experimental Demonstration of a Single-Molecule Electric Motor. *Nat. Nanotechnol.* **2011**, *6*, 625−629.
(39) Pawlak, R.; Meier, T.; Renaud, N.; Kisiel, M.; Hinaut, A.; Glatzel, T.; Sordes, D.; Durand, C.; Soe, W.-H.; Baratoff, A.; Joachim, C.; Housecroft, C. E.; Constable, E. C.; Meyer, E. Design and Characterization of an Electrically Powered Single Molecule on Gold. *ACS Nano* **2017**, *11*, 9930−9940.
(40) Henß, A.-K.; Sakong, S.; Messer, P. K.; Wiechers, J.; Schuster, R.; Lamb, D. C.; Groß, A.; Wintterlin, J. Density Fluctuations as Door-Opener for Diffusion on Crowded Surfaces. *Science* **2019**, *363*, 715−718.
(41) Patera, L. L.; Bianchini, F.; Africh, C.; Dri, C.; Soldano, G.; Mariscal, M. M.; Peressi, M.; Comelli, G. Real-Time Imaging of Adatom-Promoted Graphene Growth on Nickel. *Science* **2018**, *359*, 1243−1246.
(42) Leon, C. C.; Gunnarsson, O.; de Oteyza, D. G.; Rosławska, A.; Merino, P.; Grewal, A.; Kuhnke, K.; Kern, K. Single Photon Emission from a Plasmonic Light Source Driven by a Local Field-Induced Coulomb Blockade. *ACS Nano* **2020**, *14*, 4216−4223.
(43) Schaeverbeke, Q.; Avriller, R.; Frederiksen, T.; Pistolesi, F. Single-Photon Emission Mediated by Single-Electron Tunneling in Plasmonic Nanojunctions. *Phys. Rev. Lett.* **2019**, *123*, 246601.
(44) Parzefall, M.; Novotny, L. Optical Antennas Driven by Quantum Tunneling: A Key Issues Review. *Rep. Prog. Phys.* **2019**, *82*, 112401.
(45) Parzefall, M.; Bharadwaj, P.; Jain, A.; Taniguchi, T.; Watanabe, K.; Novotny, L. Antenna-Coupled Photon Emission from Hexagonal Boron Nitride Tunnel Junctions. *Nat. Nanotechnol.* **2015**, *10*, 1058−1063.
(46) Du, W.; Wang, T.; Chu, H.-S.; Wu, L.; Liu, R.; Sun, S.; Phua, W. K.; Wang, L.; Tomczak, N.; Nijhuis, C. A. On-Chip Molecular Electronic Plasmon Sources Based on Self-Assembled Monolayer Tunnel Junctions. *Nat. Photonics* **2016**, *10*, 274−280.
(47) Zhang, C.; Hugonin, J.-P.; Coutrot, A.-L.; Sauvan, C.; Marquier, F.; Greffet, J.-J. Antenna Surface Plasmon Emission by Inelastic Tunneling. *Nat. Commun.* **2019**, *10*, 4949.
(48) Miwa, K.; Imada, H.; Imai-Imada, M.; Kimura, K.; Galperin, M.; Kim, Y. Many-Body State Description of Single-Molecule Electroluminescence Driven by a Scanning Tunneling Microscope. *Nano Lett.* **2019**, *19*, 2803−2811.
(49) Lohrmann, A.; Iwamoto, N.; Bodrog, Z.; Castelletto, S.; Ohshima, T.; Karle, T. J.; Gali, A.; Prawer, S.; McCallum, J. C.; Johnson, B. C. Single-Photon Emitting Diode in Silicon Carbide. *Nat. Commun.* **2015**, *6*, 7783.
(50) Wei, K.; Zheng, X.; Cheng, X.; Shen, C.; Jiang, T. Observation of Ultrafast Exciton-Exciton Annihilation in CsPbBr3 Quantum Dots. *Adv. Opt. Mater.* **2016**, *4*, 1993−1997.
(51) Merino, P.; Rosławska, A.; Große, C.; Leon, C. C.; Kuhnke, K.; Kern, K. Bimodal Exciton-Plasmon Light Sources Controlled by Local Charge Carrier Injection. *Sci. Adv.* **2018**, *4*, No. eaap8349.
(52) Doppagne, B.; Chong, M. C.; Bulou, H.; Boeglin, A.; Scheurer, F.; Schull, G. Electrofluorochromism at the Single-Molecule Level. *Science* **2018**, *361*, 251−255.
(53) Hosokawa, C.; Tokailin, H.; Higashi, H.; Kusumoto, T. Transient Behavior of Organic Thin Film Electroluminescence. *Appl. Phys. Lett.* **1992**, *60*, 1220−1222.
(54) Kasemann, D.; Brückner, R.; Fröb, H.; Leo, K. Organic Light-Emitting Diodes under High Currents Explored by Transient Electroluminescence on the Nanosecond Scale. *Phys. Rev. B: Condens. Matter Mater. Phys.* **2011**, *84*, 115208.
(55) Ostroverkhova, O. Organic Optoelectronic Materials: Mechanisms and Applications. *Chem. Rev.* **2016**, *116*, 13279−13412.
(56) Kimura, K.; Miwa, K.; Imada, H.; Imai-Imada, M.; Kawahara, S.; Takeya, J.; Kawai, M.; Galperin, M.; Kim, Y. Selective Triplet Exciton Formation in a Single Molecule. *Nature* **2019**, *570*, 210−213.
(57) Chen, G.; Luo, Y.; Gao, H.; Jiang, J.; Yu, Y.; Zhang, L.; Zhang, Y.; Li, X.; Zhang, Z.; Dong, Z. Spin-Triplet-Mediated Up-Conversion and Crossover Behavior in Single-Molecule Electroluminescence. *Phys. Rev. Lett.* **2019**, *122*, 177401.
(58) Moreau, E.; Robert, I.; Manin, L.; Thierry-Mieg, V.; Gérard, J. M.; Abram, I. Quantum Cascade of Photons in Semiconductor Quantum Dots. *Phys. Rev. Lett.* **2001**, *87*, 183601.
(59) Zhang, Y.; Meng, Q.-S.; Zhang, L.; Luo, Y.; Yu, Y.-J.; Yang, B.; Zhang, Y.; Esteban, R.; Aizpurua, J.; Luo, Y.; Yang, J.-L.; Dong, Z.-C.; Hou, J. G. Sub-Nanometre Control of the Coherent Interaction Between a Single Molecule and a Plasmonic Nanocavity. *Nat. Commun.* **2017**, *8*, 15225.
(60) Imada, H.; Miwa, K.; Imai-Imada, M.; Kawahara, S.; Kimura, K.; Kim, Y. Single-Molecule Investigation of Energy Dynamics in a Coupled Plasmon-Exciton System. *Phys. Rev. Lett.* **2017**, *119*, 013901.
(61) Kröger, J.; Doppagne, B.; Scheurer, F.; Schull, G. Fano Description of Single-Hydrocarbon Fluorescence Excited by a Scanning Tunneling Microscope. *Nano Lett.* **2018**, *18*, 3407−3413.
(62) Chikkaraddy, R.; de Nijs, B.; Benz, F.; Barrow, S. J.; Scherman, O. A.; Rosta, E.; Demetriadou, A.; Fox, P.; Hess, O.; Baumberg, J. J. Single-Molecule Strong Coupling at Room Temperature in Plasmonic Nanocavities. *Nature* **2016**, *535*, 127−130.

https://dx.doi.org/10.1021/acsnano.0c03704
ACS Nano 2020, 14, 6366−6375

(63) Flagg, E. B.; Muller, A.; Robertson, J. W.; Founta, S.; Deppe, D. G.; Xiao, M.; Ma, W.; Salamo, G. J.; Shih, C. K. Resonantly Driven Coherent Oscillations in a Solid-State Quantum Emitter. *Nat. Phys.* **2009**, *5*, 203−207.
(64) van der Ende, B. M.; Aarts, L.; Meijerink, A. Near-Infrared Quantum Cutting for Photovoltaics. *Adv. Mater.* **2009**, *21*, 3073−3077.
(65) Loth, S.; Etzkorn, M.; Lutz, C. P.; Eigler, D. M.; Heinrich, A. J. Measurement of Fast Electron Spin Relaxation Times with Atomic Resolution. *Science* **2010**, *329*, 1628−1630.
(66) Zhang, Y.; Luo, Y.; Zhang, Y.; Yu, Y.-J.; Kuang, Y.-M.; Zhang, L.; Meng, Q.-S.; Luo, Y.; Yang, J.-L.; Dong, Z.-C.; Hou, J. G. Visualizing Coherent Intermolecular Dipole-Dipole Coupling in Real Space. *Nature* **2016**, *531*, 623−627.
(67) Luo, Y.; Chen, G.; Zhang, Y.; Zhang, L.; Yu, Y.; Kong, F.; Tian, X.; Zhang, Y.; Shan, C.; Luo, Y.; Yang, J.; Sandoghdar, V.; Dong, Z.; Hou, J. G. Electrically Driven Single-Photon Superradiance from Molecular Chains in a Plasmonic Nanocavity. *Phys. Rev. Lett.* **2019**, *122*, 233901.
(68) Hettich, C.; Schmitt, C.; Zitzmann, J.; Kühn, S.; Gerhardt, I.; Sandoghdar, V. Nanometer Resolution and Coherent Optical Dipole Coupling of Two Individual Molecules. *Science* **2002**, *298*, 385−389.
(69) Wang, D.; Kelkar, H.; Martin-Cano, D.; Rattenbacher, D.; Shkarin, A.; Utikal, T.; Götzinger, S.; Sandoghdar, V. Turning a Molecule into a Coherent Two-Level Quantum System. *Nat. Phys.* **2019**, *15*, 483−489.
(70) Koperski, M.; Nogajewski, K.; Arora, A.; Cherkez, V.; Mallet, P.; Veuillen, J.-Y.; Marcus, J.; Kossacki, P.; Potemski, M. Single Photon Emitters in Exfoliated WSe_2 Structures. *Nat. Nanotechnol.* **2015**, *10*, 503−506.
(71) Srivastava, A.; Sidler, M.; Allain, A. V.; Lembke, D. S.; Kis, A.; Imamoğlu, A. Optically Active Quantum Dots in Monolayer WSe_2. *Nat. Nanotechnol.* **2015**, *10*, 491−496.
(72) Tran, T. T.; Bray, K.; Ford, M. J.; Toth, M.; Aharonovich, I. Quantum Emission from Hexagonal Boron Nitride Monolayers. *Nat. Nanotechnol.* **2016**, *11*, 37−41.
(73) Pommier, D.; Bretel, R.; López, L. E. P.; Fabre, F.; Mayne, A.; Boer-Duchemin, E.; Dujardin, G.; Schull, G.; Berciaud, S.; Le Moal, E. Scanning Tunneling Microscope-Induced Excitonic Luminescence of a Two-Dimensional Semiconductor. *Phys. Rev. Lett.* **2019**, *123*, 027402.
(74) Schuler, B.; Cochrane, K. A.; Kastl, C.; Barnard, E.; Wong, E.; Borys, N.; Schwartzberg, A. M.; Ogletree, D. F.; de Abajo, F. J. G.; Weber-Bargioni, A. Electrically Driven Photon Emission from Individual Atomic Defects in Monolayer WS2. *arXiv (Mesoscale and Nanoscale Physics)*, October 10, 2019, 191004612, ver. 1. https://arxiv.org/abs/1910.04612 (accessed October 10, 2019).
(75) Krane, N.; Lotze, C.; Läger, J. M.; Reecht, G.; Franke, K. J. Electronic Structure and Luminescence of Quasi-Freestanding MoS_2 Nanopatches on Au(111). *Nano Lett.* **2016**, *16*, 5163−5168.
(76) Wickenburg, S.; Lu, J.; Lischner, J.; Tsai, H.-Z.; Omrani, A. A.; Riss, A.; Karrasch, C.; Bradley, A.; Jung, H. S.; Khajeh, R.; Wong, D.; Watanabe, K.; Taniguchi, T.; Zettl, A.; Neto, A.H. C.; Louie, S. G.; Crommie, M. F. Tuning Charge and Correlation Effects for a Single Molecule on a Graphene Device. *Nat. Commun.* **2016**, *7*, 13553.
(77) Rosławska, A. M. Dynamics of Nanoscale Systems Probed by Time-Resolved STM-Induced Luminescence. *Ph.D. Thesis*, École Polytechnique Fédérale de Lausanne, Lausanne, Switzerland, 2019.
(78) Benz, F.; Schmidt, M. K.; Dreismann, A.; Chikkaraddy, R.; Zhang, Y.; Demetriadou, A.; Carnegie, C.; Ohadi, H.; de Nijs, B.; Esteban, R.; Aizpurua, J.; Baumberg, J. J. Single-Molecule Optomechanics in "Picocavities. *Science* **2016**, *354*, 726−729.
(79) Kuzucu, O.; Wong, F. N. C.; Kurimura, S.; Tovstonog, S. Joint Temporal Density Measurements for Two-Photon State Characterization. *Phys. Rev. Lett.* **2008**, *101*, 153602.
(80) Allgaier, M.; Vigh, G.; Ansari, V.; Eigner, C.; Quiring, V.; Ricken, R.; Brecht, B.; Silberhorn, C. Fast Time-Domain Measurements on Telecom Single Photons. *Quantum Sci. Technol.* **2017**, *2*, 034012.
(81) Hong, C. K.; Ou, Z. Y.; Mandel, L. Measurement of Subpicosecond Time Intervals between Two Photons by Interference. *Phys. Rev. Lett.* **1987**, *59*, 2044−2046.
(82) Lyons, A.; Knee, G. C.; Bolduc, E.; Roger, T.; Leach, J.; Gauger, E. M.; Faccio, D. Attosecond-Resolution Hong-Ou-Mandel Interferometry. *Sci. Adv.* **2018**, *4*, No. eaap9416.

https://dx.doi.org/10.1021/acsnano.0c03704
ACS Nano 2020, 14, 6366−6375